

Preparation of highly hydrophobic PVDF hollow fiber composite membrane with lotus leaf-like surface and its desalination properties

Hongbin Li^{1, 2}, Xingchen Zi¹, Wenying Shi^{*1, 2}, Longwei Qin¹, Haixia Zhang¹ and Xiaohong Qin^{1, 3}

¹School of Textiles Engineering, Henan University of Engineering, 1 Xianghe Road, Zhengzhou 450007, P. R. China

²Collaborative Innovation Center of Textile and Garment Industry of Henan Province, 41 Zhongyuan Road, Zhengzhou 450007, P. R. China

³School of Textiles Science, Donghua University, 2999 North Renmin Road, Shanghai 201620, P. R. China

(Received August 16, 2018, Revised March 16, 2019, Accepted March 20, 2019)

Abstract. Lotus leaf has a special dual micro and nano surface structure which gives its highly hydrophobic surface characteristics and so-called self cleaning effect. In order to endow PVDF hollow fiber membrane with this special structure and improve the hydrophobicity of membrane surface, PVDF hollow fiber composite membranes was obtained through the immersion coating of poly(vinylidene fluoride-co-hexafluoropropylene) (PVDF-HFP) dilute solution on the outside surface of PVDF support membrane. The prepared PVDF composite membranes were used in the vacuum membrane distillation (VMD) for the desalination. The effects of PVDF-HFP dilute solution concentration in the dope solution and coating time on VMD separation performance was studied. Membranes were characterized by SEM, WCA measurement, porosity, and liquid entry pressure of water. VMD test was carried out using 35 gL⁻¹ NaCl aqueous solution as the feed solution at feed temperature of 30 °C and the permeate pressure of 31.3 kPa. The vapour flux reached a maximum when PVDF-HFP concentration in the dilute solution was 5 wt% and the coating time was kept in the range of 10-60 s. This was attributed to the well configuration of micro-nano rods which was similar with the dual micro-nano structure on the lotus leaf. Compared with the original PVDF membrane, the salt rejection can be well maintained which was greater than 99.99 % meanwhile permeation water conductivity was kept at a low value of 7-9 μS cm⁻¹ during the continuous testing for 360 h.

Keywords: hydrophobicity; PVDF; hollow fiber membrane; vacuum membrane distillation; desalination

1. Introduction

In the last years, the desalination of seawater and brackish water to obtain fresh water in arid regions has gained a growing interest to overcome the problem of water shortage. Compared with the conventional desalination technology-reverse osmosis (RO), membrane distillation (MD) with higher separation efficiency, milder operating conditions, and lower energy consumption has exhibited promising application in seawater and brackish desalination, heavy metal removal, wastewater treatment and various separation processes (Pangarkar *et al.* 2018, Edwie *et al.* 2012).

Compared with other MD configurations, VMD can provide greater mass transfer driven force and therefore produce higher vapor flux across the separation membrane (Racz *et al.* 2015). In addition to the optimization of the operating conditions in the VMD process, membrane materials are the key determinants of VMD performance. Membrane types include flat sheet, hollow fiber, capillary and spiral-wound. Among them, hollow fiber membranes are widely used in VMD because of their high packing density, self-supporting structure and high degree of modularity (Fang *et al.* 2012). In VMD, with the exception

of the good mechanical strength, heat resistance and chemical stability, hydrophobicity is one of the basic characteristics of the hollow fiber membrane which determines the wettability of the membrane surface. The vapor pressure difference requires a non-wetting porous hydrophobic membrane to assure the strong driven force for mass transfer.

Several types of polymers have been studied and applied in the preparation of hydrophobic membrane in VMD process because of their low surface energies, high chemical resistance, thermal stability, good mechanical strengths and processability (Loussif *et al.* 2016). The most used hydrophobic materials in VMD are fluorinated polymers, including polyvinylidene fluoride (PVDF) (Kim *et al.* 2017, Chang *et al.* 2014), polytetrafluoroethylene (PTFE) (Guo *et al.* 2017) and polyolefin polymers, such as polypropylene (PP) (Gryta *et al.* 2013) and polyethylene (PE) (Xu *et al.* 2015) and so on. Among them, PVDF is the most widely used in VMD investigations. Some researches have been centered on the studies of the development of novel hydrophobic membrane material such as poly(phthalazinone ether sulfone ketone) (PPESK) (Jin *et al.* 2008) and poly(tetrafluoroethylene-co-hexafluoropropylene) (FEP) (Chen *et al.* 2015), the changes in the membrane formation process such as thermally induced phase separation (TIPS), nonsolvent induced phase separation (NIPS) (Wu *et al.* 2006, Zuo *et al.* 2017b, Zuo *et al.* 2017a, Tang *et al.* 2012), cold pressing method (Zhu *et al.* 2013) and vapour induced phase separation (VIPs), the

*Corresponding author, Professor
E-mail: shiwenyinggg@126.com

structure optimization of PVDF hollow fiber membranes (Drioli *et al.* 2013), and the development of robust multi-bore PVDF hollow fiber membrane (Lu *et al.* 2016, Chang *et al.* 2019). Besides, as one simple and high-efficiency membrane preparation method, the hydrophobicity modification of PVDF hollow fiber membrane has become a hot research topic of the PVDF membrane in VMD. Various membrane modification techniques have been reported, including chemical grafting (Fang *et al.* 2012), blending (Teoh *et al.* 2009, Wang *et al.* 2016) and surface omniphobic coating (Lu *et al.* 2018). Surface coating of a highly hydrophobic layer on the available PVDF hollow fiber membrane is a simple and effective way to obtain hydrophobic composite membranes. In this method, the coating substance plays an important role in determining the final properties of the composite membranes. Some hydrophobic substances have been successfully coated on hollow fiber membranes, such as polytrifluoropropylsiloxane (Jin *et al.* 2018), silicone rubber (Jin *et al.* 2018), copolymer (Hyflon AD60) of tetrafluoroethylene (TFE) and 2,2,4-trifluoro-5-trifluoromethoxy-1,3-dioxole (TTD) (Tong *et al.* 2016), and nanoparticles such as nanosilica (Xu *et al.* 2017) and nano titanium dioxide (Meng *et al.* 2014).

Lotus leaf has a special dual micro and nano surface structure which gives its highly hydrophobic surface characteristics and so-called self cleaning effect. In recent years, the studies of lotus leaf-like surface structure are concentrated on the enrichment of nanoparticles, such as nano zinc oxide (ZnO) (Ameen *et al.* 2016), nickel (Ni) (Shafiei *et al.* 2009), aluminum (Kim *et al.* 2012), carbon nanotube (Chen *et al.* 2018), etc. Some researchers use the polymer to simulate the surface structure of lotus leaf and apply the special structure in hydrophobic separation membrane. The etching method of PVDF particles combined with an ultrafiltration coating process was employed to hydrophobically modify the porous PVDF hollow fiber membranes (Yan *et al.* 2017). The prepared PVDF hollow fiber membrane with a superhydrophobic lotus leaf-like surface was applied in direct contact membrane distillation (DCMD) process for desalination. Another coating way to obtain the hydrophobic lotus leaf-like membrane surfaces was the chemical vapor deposition of the hydrophobic substance such methyltrichlorosilane (MTS) on the support membrane surfaces (Zheng *et al.* 2009). The superhydrophobic PVDF hollow fiber membrane was also directly obtained through the changes of vapor-induced phase-separation (VIPS) process with a long-time exposure in a saturated moist air (Peng *et al.* 2012a, Peng *et al.* 2012b).

In recent years, relevant scholars have also tried various methods of polymer synthesis and new membrane formation processes in order to broaden the source of hydrophobic hollow fiber membrane materials, such as PVDF copolymers (PVDF-co-hexafluoropropylene (PVDF-HFP) (Khayet *et al.* 2012), PVDF-co-trifluorochloroethylene (PVDF-CTFE) (Wang *et al.* 2016) and PVDF-co-hexafluoropropylene (PVDF-FEP) (Chen *et al.* 2015), fluorinated polyoxadiazole (f-POD) (Xu *et al.* 2018)). Among them, the copolymer PVDF-HFP has higher

hydrophobicity, higher solubility, lower crystallinity which is due to the incorporation of an amorphous phase of fluoropropylene (HFP) into the main constituent vinylidene fluoride (VDF) blocks. Professor Khayet's research group has made a continuous and systematic study on the preparation of PVDF-HFP hollow fiber membranes by nonsolvent induced phase separation (NIPS) and their application in MD from 2009 to 2017. Firstly, the effects of PVDF-HFP concentration in spinning solution on the micropore structure, pore size (García-Payo *et al.* 2010) and liquid entry pressure (LEP) (García-Payo *et al.* 2009) of hollow fiber membranes were investigated. Then, seven spinning parameters (including PVDF-HFP concentration, the additive concentration, dry distance, core liquid and external coagulation bath temperature, core liquid flow rate, winding rate and extrusion pressure) in PVDF-HFP spinning process were strictly designed and analyzed by using partial factor design method (Khayet *et al.* 2012). Afterwards, the effect of different solvents on the structure and properties of PVDF-HFP hollow fiber membranes was studied (García-Payo *et al.* 2014). And the effect of core liquid and external coagulation bath on the structure and MD properties of PVDF-HFP membrane was also studied by the thermodynamic and dynamic properties of PVDF-HFP membrane (García-Payo *et al.* 2017a, García-Payo *et al.* 2017b).

In the present work, in order to improve membrane surface hydrophobicity, PVDF hollow fiber composite membranes were prepared through the coating of dilute solution on the outside surface of PVDF hollow fiber membrane. It is well known that the polymer concentration of porous separation membranes prepared by phase inversion is generally higher than 10 wt% in order to achieve the rheological properties required for membrane casting of hollow fiber membrane spinning. In this study, the coating solution used is the hydrophobic PVDF-HFP dilute solution with a very low polymer concentration (3-7 wt%). The phase inversion of the dilute solution is not a continuous phase separation process, but a local phase separation. This would result in the formation of a particulate bulge structure on the outer surface of the hollow fiber support membrane. The highly hydrophobic PVDF-HFP which had good compatibility with PVDF was chosen as the hydrophobic polymer candidate in dilute solution. The prepared PVDF membranes were used in the vacuum membrane distillation (VMD) for the desalination. The effect of the concentration of PVDF-HFP dilute solution in the dope solution and coating time on the separation performance in VMD was studied. The prepared PVDF membranes were characterized by scanning electronic microscopy (SEM), water contact angle (WCA) measurement, porosity, and liquid entry pressure of water.

2. Experimental

2.1 Materials

Poly(vinylidene fluoride) (PVDF, FR-904) powder was supplied as resin powder from Shanghai 3F New Materials Co., Ltd., China and dried in a vacuum oven at 80°C for 12h

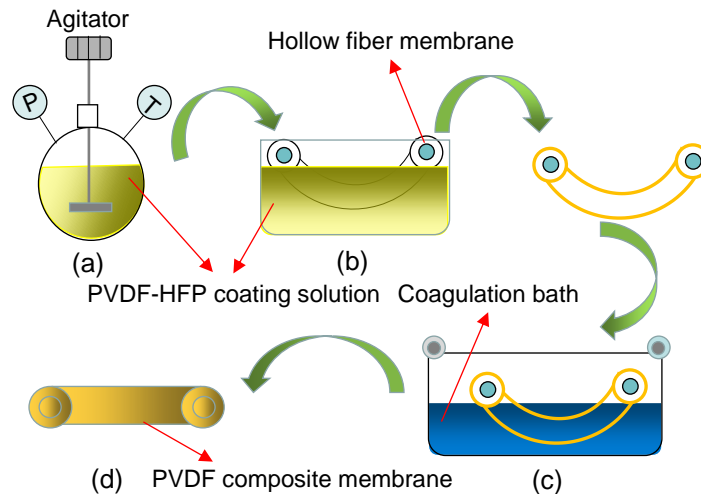


Fig. 1 Schematic diagram of the preparation of PVDF hollow fiber composite membrane

before use. Polyvinylidene fluoride-co-hexafluoropropylene (PVDF-HFP, $M_w=455,000 \text{ g}\cdot\text{mol}^{-1}$) were purchased from Sigma-Aldrich. Polyethylene glycol (PEG, $M_w=60,000$ and 400), *N,N*-dimethylformamide (DMF) and *N,N*-dimethylacetamide (DMAc) were obtained by Tianjin Kemiou reagent Co., Ltd. (China). Lithium chloride (LiCl) and sodium chloride (NaCl) were analytical grade and supplied by Aladdin Industrial Corporation (Shanghai, China) and used without further purification.

2.2 Preparation of PVDF hollow fiber composite membrane

PVDF hollow fiber composite membranes were prepared through the coating of PVDF-HFP dilute solution on the outside surface of PVDF hollow fiber support membrane. The schematic diagram of the preparation of PVDF hollow fiber composite membrane was illustrated in Fig. 1. PVDF support membrane was fabricated via the dry-wet spinning technique. The spinning solution was composed of PVDF (17 wt%), LiCl (1 wt%), PEG-60,000 granules (6 wt%) and DMAc (76 wt%). The spinning solution was extruded via a tube in-orifice spinneret with inner/outer diameters of 0.8/1.3 mm using ultrafiltration water and pure water as the coagulation bath and bore liquid, respectively. The prepared PVDF hollow fiber support membrane was designated as 0#.

The dilute solution containing the certain content of PVDF-HFP and DMF, and PEG-400 was stirred at 50 °C until a homogeneous solution was obtained as illustrated in Fig. 1(a). Because the concentration of polymer PVDF-HFP in dilute solution was very low (3–7 wt%), PEG-400 with a high amount of 33 wt% was added into the dilute solution to ensure that dilute solution has a certain viscosity to facilitate subsequent coating and phase inversion processes. The specific compositions of the coating solution corresponding to the membrane samples 1#–4# were presented in Table 1. The ends of PVDF hollow fiber support membrane treated by the gradient pore protection were sealed with the silicone rubber and immersed in the PVDF-HFP coating solution for a certain time (Fig. 1(b)).

Table 1 Compositions of the PVDF-HFP coating solution

Membrane Sample	PVDF-HFP (wt%)	PEG-400 (wt%)	DMF (wt%)
1#	3	33	64
2#	5	33	62
3#	7	33	60
4#	9	33	58

Then, PVDF support membrane was immediately taken out and immersed into the coagulation bath for 1 h (Fig. 1(c)). Afterwards, the nascent PVDF composite membrane was washed with pure water for several times and preserved in pure water. Finally, the PVDF composite membrane was obtained (Fig. 1(d)).

2.3 Characterization of membrane morphology and structure

The morphology of the hollow fiber membranes was observed by a field emission scanning electronic microscopy (SEM, FEI Quanta 250, USA). Prior to SEM observation, the dry hollow fiber membrane samples were immersed in liquid nitrogen and fractured, and then sputtered with gold. The surface of each hollow fiber membrane was analyzed for its hydrophobicity by measuring the water contact angle (WCA) on a Kruss Instrument (CM3250-DS3210, Germany) at ambient temperature. 1 μL water droplet was dropped on the membrane surface using a micro syringe and then the WCA was measured. The images were captured by a camera. The measurements were carried out on at least five spots and the average was obtained.

During MD process, membrane porosity plays an important role on the MD performance (Alkudhiri *et al.* 2012). Porous structure means that water vapor can pass through the membrane channel quickly and the mass transfer rate can be effectively increased in MD process. On the other hand, high porosity can reduce the thermal conductivity of membrane material itself, thereby improving the heat transfer efficiency. Thus, the porosities

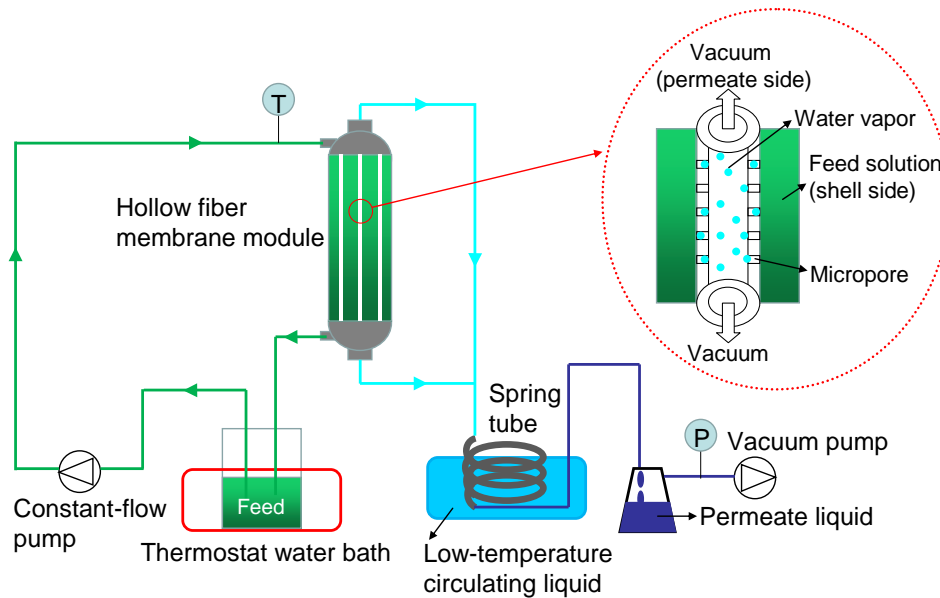


Fig. 2 Flow diagram of the vacuum membrane distillation

of membrane before and after coating modification were obtained through the weight difference method according to Eq. (1).

$$\varepsilon = \frac{W_w - W_d}{Al\rho} \quad (1)$$

where W_w and W_d were the weight of wet and dry membranes (g), respectively. A , l , and ρ were the sample area (cm^2), the length of hollow fiber membrane (cm) and water density at atmosphere temperature ($\text{g}\cdot\text{cm}^{-3}$), successively.

To eliminate the negative effect of membrane pore wetting on VMD performance, membrane material used in the MD must be hydrophobic. However, pore wetting will commonly occur and hence the quality of the production water may be deteriorated if the applied transmembrane hydrostatic pressure exceeds the liquid entry pressure of water (LEP_w) (Tong *et al.* 2016). LEP_w is defined as the minimum pressure that admits the aqueous solution to penetrate into membrane pores. For determining LEP_w , hollow fiber membranes were mounted in tubular stainless steel modules. The shell side was filled with water, and a slight pressure was introduced from the compressed nitrogen, and increased with a step of 5 kPa at an interval of 5 min until the first water droplet permeated on the fiber lumen side. The corresponding pressure was determined as the LEP_w of the membrane sample. Capillary flow porometry was used to determine the pore sizes in the microporous membranes. membrane sample was wetted in a fluid (Porwick, proprietary product of PMI, surface tension 18 dyn/cm) and sealed in a chamber for the measurement.

2.4 Vacuum membrane distillation experiments

Vacuum membrane distillation (VMD) experiments were carried out to evaluate the performance of the PVDF hollow fiber composite membranes. The experimental set-

up used for vacuum membrane distillation was shown in Fig. 2. The feed solution was introduced in the shell side of the hollow fiber membrane modules by a constant-flow pump. Vacuum was applied on the lumen of hollow fiber membrane through a vacuum pump. The water vapors permeated through membrane micropores and were condensed into liquid water after subsequent condensation by a stainless steel spring tube. The spring tube was surrounded by a low-temperature circulating liquid at 15°C below zero.

The feed chamber was maintained at 50°C with the use of a thermostat water bath under magnetic agitation to minimise temperature polarization effects. The permeate pressure was kept at 31.3 kPa so that the permeated water vapour could be easily collected. $35\text{ g}\cdot\text{L}^{-1}$ NaCl aqueous solution was used as the feed solution to mimic sea water. The distillate collected after a specific interval of time was weighted and the flux was calculated according to the following equation. The salt concentrations were examined via a conductivity meter (DDS-11A, Shanghai Leici Instrument Works, China). NaCl rejection (R) and membrane permeate water flux (J_w) were calculated as Eqs. (2) and (3). Each data was obtained by averaging the records of five tests to ensure the accuracy of the data.

$$R = \left(1 - \frac{C_p}{C_f}\right) \times 100\% \quad (2)$$

where C_p and C_f were NaCl concentrations in the permeate and feed solution, respectively.

$$J_w = \frac{m}{A_o \times t} \quad (3)$$

where m , A_o and t were permeate water volume (L), the effective outside area of hollow fiber membrane (m^2) and filtration time (h), respectively.

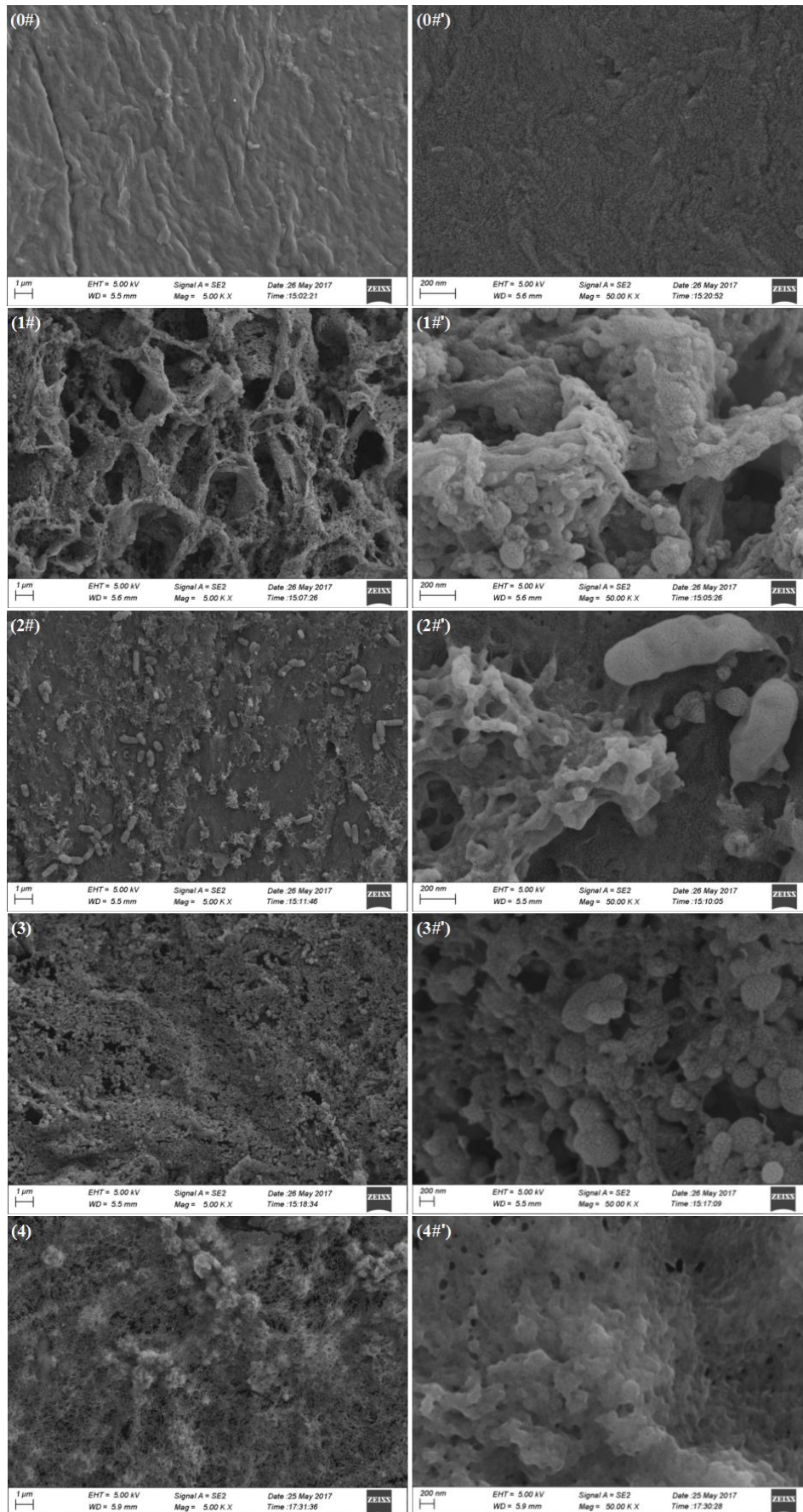


Fig. 3 Outside surface SEM images of different PVDF hollow fiber membranes (0#-4#) and the corresponding magnification images (0#'-4#')

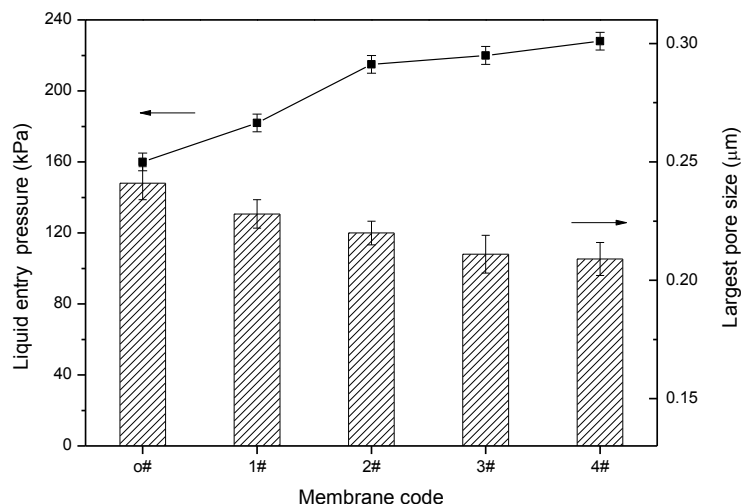


Fig. 4 Liquid entry pressure and largest pore size of different PVDF membranes

3. Results and discussion

3.1 Morphology of different PVDF hollow fiber membranes

Fig. 3 showed the outside surface SEM images of different PVDF hollow fiber membranes. It could be seen from Fig. 3(0#) that the outside surface of the original PVDF membrane was relatively smooth with a few wrinkles. After the coating of PVDF-HFP dilute solution, lots of uneven bulges and cavities initially emerged on PVDF membrane surface as shown in Fig. 3(1#). Through the observation of Fig. 3(1#), these bulges were composed of many nanoscale globular particles. With the increase of PVDF-HFP concentration in the coating solution, a large number of semi-continuous structures appeared on the surface of the PVDF membrane (Fig. 3(2#)), and there were many rods with a length of about 1 microns and a diameter of about 200 nm. With the further increase of PVDF-HFP concentration, these semi-continuous structures are gradually connected to a continuous membrane structure, and there are still some rods on the PVDF membrane surface (Fig. 3(3#)). As the PVDF-HFP content continues to increase, the complete dense membrane structure was formed and became dense with a few irregular ridges as shown in Fig. 3(4#).

The polymer concentration in this study was much lower than that in the conventional phase inversion process. Because the instantaneous phase separation dominated the membrane formation process, the continuous membrane structure could not be formed under lower polymer (PVDF-HFP) concentration after the exchange between solvent and non-solvent. And only some discontinuous fragmentation structures appeared (Fig. 3(1#)). At the appropriate PVDF-HFP concentration, the polymer dilute solution was coagulated with the local formation of many gel nuclei. As the polymer concentration was very low, the further growth of gel nuclei could not form a continuous membrane structure, which led to the emergence of a large number of micron rods (Fig. 3(2#)). When the polymer concentration

continued to increase, a continuous membrane structure could be obtained (Fig. 3(3#) and (4#)).

3.2 Structure parameters of different PVDF membranes

Fig. 4 showed the liquid entry pressure of water (LEP_w) and largest pore size of different PVDF membranes. It could be seen with the increase of PVDF-HFP content in the dilute solution, the liquid entry pressure gradually increase from 160 kPa of the neat PVDF membrane to 223 kPa of the 4# PVDF composite membrane. And the largest pore size showed the opposite trend with the decrease from 0.232 μm of the neat PVDF membrane to 0.20 μm of the 4# PVDF composite membrane as shown in Fig. 4. The feed can penetrate the membrane pores and the quality of the permeate water will be deteriorated if a transmembrane hydrostatic pressure is higher than the liquid entry pressure of water (LEP_w). LEP_w is a significant membrane structure parameter which characterizes the antiwetting properties of hydrophobic membrane and its value depends on the pore size and membrane hydrophobicity (Tong *et al.* 2016). Membrane with a high hydrophobic surface and a small pore size would show a high value of LEP_w . As shown in Fig. 4, the gradually decline of membrane largest pore size was favorable for the increase of LEP_w . Besides, the enhancement of membrane surface hydrophobicity as confirmed in the WCA measurement also facilitated the improvement of membrane antiwetting properties. The data of LEP_w reported in the published works were listed in Table 2. It could be found that among the 11 literatures with data records, there are 4, 1, 4 and 2 literatures reported LEP_w values below 100 kPa, 100-200 kPa, 200-300 kPa and 300 kPa respectively. The LEP_w value of PVDF hollow fiber composite membrane prepared in this work is moderate.

During MD process, high membrane porosity plays an important role in the MD performance (Alkudhiri *et al.* 2012). Thus, it is important to keep high porosity during coating modification. The porosities of resulted PVDF

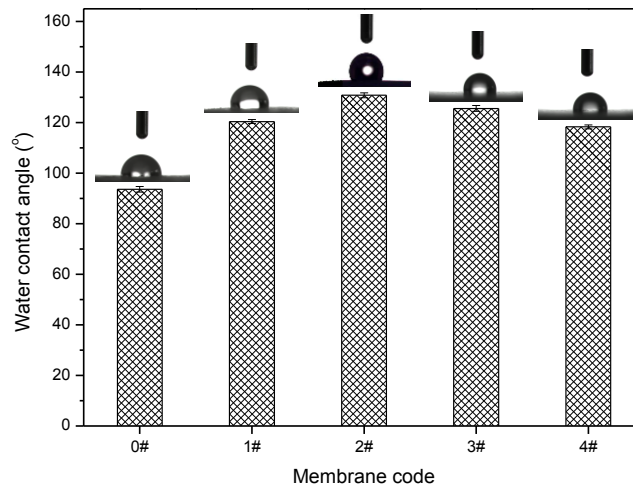


Fig. 5 Static water contact angle (WCA) of the outside surface of different PVDF membranes

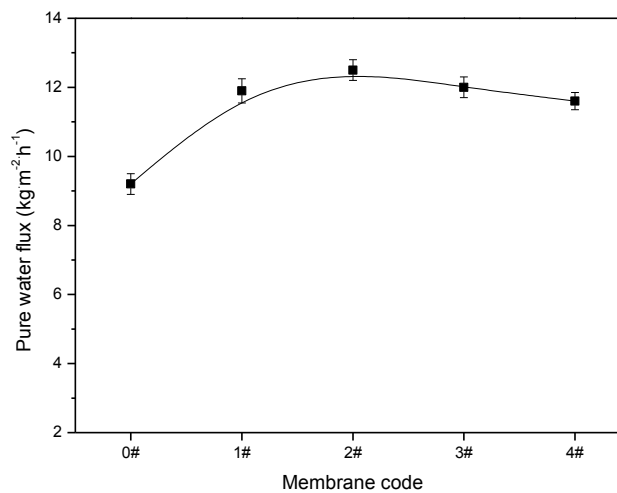


Fig. 6 Variations of pure water flux of different PVDF hollow fiber membranes

composite membranes were in the ranged of 61 %-62 % which had no obvious difference between the original PVDF (62.1 %) and membrane composite membrane. This indicated that the coating just affected the surface of PVDF hollow fiber membrane without the penetration of PVDF-HFP into membrane pores below.

3.3 Hydrophilicity of membrane surface

Static water contact angle (WCA) was measured to evaluate the hydrophobicity of different PVDF hollow fiber membrane surface. The data were shown in Fig. 5. It could obviously seen that the WCA values of all PVDF composite membranes were higher than that of the original PVDF membrane. This implied that the coating of PVDF-HFP dilute solution could improve membrane surface hydrophobicity. It can be referred by the Wenzel equation that the WCA of a hydrophobic surface ($\theta > 90^\circ$) will increase with an increase of surface roughness. As observed from the SEM images in Fig. 3, after the PVDF-HFP coating, membrane surface emerged lots of globular particles and rod-like bulges which increase the surface

roughness and hence facilitated the hydrophobicity enhancement.

In addition, it could be seen from Fig. 5 that with the increase of PVDF-HFP content in the dilute solution, the WCA value initially increased and then slightly decreased with a maximum of 130.8° for 2# composite membrane. There are two major factors affecting the WCA value including the membrane surface structure and intrinsic wettability of the material itself (Ganesh *et al.* 2013, Li *et al.* 2017). Compared with PVDF, the hydrophobicity of PVDF-HFP molecule itself increased the WCA of the composite membrane surface. Besides, the difference in the surface structure of different PVDF composite membranes also caused the changes of membrane surface hydrophobicity. It could be seen from the SEM images that a large number of micronscale rods and their surrounding nanoscale semi-continuous structure emerged on 2# membrane surface which were similar to the dual micro-nano structure on the lotus leaf surface and hence resulted in the obvious enhancement of membrane surface hydrophobicity. By comparison of 2# and other composite membranes, the simultaneous appearance of large amounts of the micronscale rods and nanoscale semi-continuous

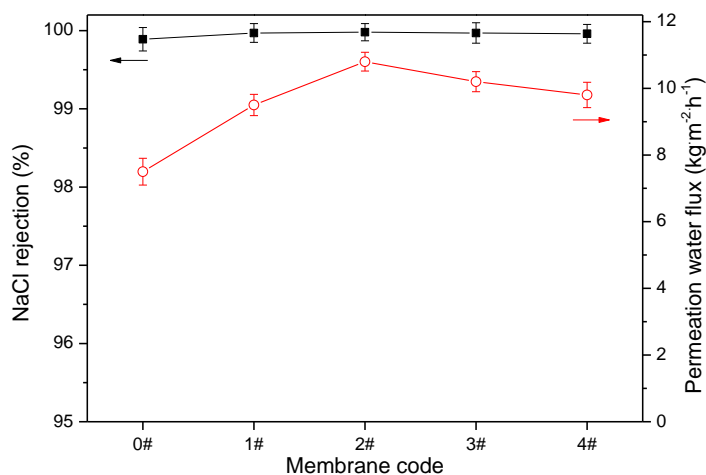


Fig. 7 Variations of separation performance of different PVDF hollow fiber membranes

structure would improve membrane surface hydrophobicity. Therefore, when PVDF-HFP concentration in the dilute solution was 5 wt%, the surface hydrophobicity of PVDF composite membrane (2#) reached the strongest. The highly hydrophobicity was favorable for the enhancement of membrane permeation flux during the membrane distillation process.

3.4 Pure water flux of different PVDF membranes

The effect of PVDF-HFP concentration in the dilute solution on the pure water flux of different PVDF hollow fiber membranes was shown in Fig. 6. It could be seen that the pure water flux increased upon the PVDF-HFP coating from 0# to 2# and as the PVDF-HFP concentration in the dilute solution further increased, the pure water flux had a slight decrease with a maximum value of 12.5 kg·m⁻²·h⁻¹ for 2# membrane. This trend was in accordance with the variations of WCA measurements in Fig. 5.

When the PVDF-HFP concentration was low, the gradual formation of the micro-nano structure on PVDF hollow fiber membrane enhanced membrane hydrophobicity which reduced the adhesive of water molecular to membrane surface, so that the liquid film along the outside surface of PVDF hollow fiber composite membrane could be effectively inhibited. And hence the bound layer thickness of temperature polarization and mass transfer decreased (Drioli *et al.* 2013). This is beneficial for increasing the MD permeability. Because of the special structure and hydrophobicity of the outside surface of PVDF composite membrane, water molecules could keep the spherical structure. The evaporation, diffusion and condensation could be well driven by the difference of heat and pressure. By comparison, the outside surface of the original PVDF membrane was relatively smooth and less hydrophobic, and water molecules were prone to wetting on membrane surface and formed a thin liquid film, which resulted in the increase of mass transfer resistance of water molecules followed by a lower water flux as shown in Fig. 6. When the PVDF-HFP concentration was high, the formation of the relative dense membrane on PVDF support

membrane and the declined pore size of the PVDF composite membrane as shown in Fig. 4 increased mass transfer resistance (Tong *et al.* 2016). Consequently, the pure water flux slightly decreased.

3.5 Separation performance of different PVDF hollow fiber membranes

The separation performance including membrane permeability and the NaCl rejection were measured and the results of were presented in Fig. 7. It could be seen that the permeation water flux increased initially and afterwards declined slowly with a maximum value for 2# PVDF membrane. The NaCl rejection of different PVDF hollow fiber membranes were around 99.9 % and nearly had no difference.

In order to make a clear comparison of desalination conditions, the conductivity data of water produced by different PVDF membranes after the distillation of mimic seawater were shown in Fig. 8. The conductivity of the mimic seawater (35 g·L⁻¹ NaCl aqueous solution) was 510 mS·cm⁻¹. Although the NaCl rejection was about 99.9 %, the production water conductivity of different PVDF hollow fiber membranes was obviously different. These results were mainly due to the difference of surface structure and hydrophobicity between different membranes. The outside surface of PVDF composite membrane with the special structure and hydrophobicity was difficult to wetting and the mass transfer process could be well carried on. However, water molecules were prone to wetting on the original PVDF membrane surface and formed a thin liquid film which resulted in the increase of mass transfer resistance of water molecules followed by a lower water flux. Some solutes of NaCl could permeate the lumen side of PVDF hollow fiber membrane which contributed to the enlargement of the production water conductivity in Fig. 8.

Table 2 listed the comparison between the current work and other VMD membranes in terms of water contact angle (WCA), salt rejection (*R*) and permeation water flux (*J_w*). It could be seen that salt rejection of most of the membranes in VMD reported in previous literatures was over 99 % and

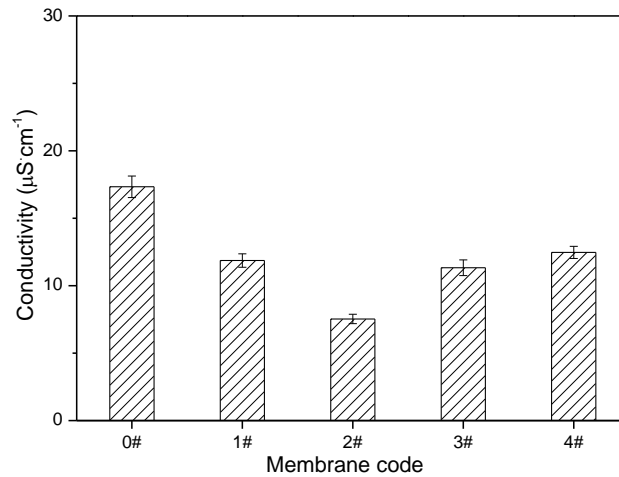


Fig. 8 The production water conductivity of different PVDF hollow fiber membranes

Table 2 A comparison of membrane properties and VMD performance with previous literature data

Membrane	Preparation method	Feed condition	Feed temperature (°C)	Permeate pressure	LEP_w (kPa)	WCA (°)	R (%)	J_w (kg m ⁻² h ⁻¹)	Ref.
PP (a)	Commercial product	1.152 wt% NaCl	80	-0.08 Mpa	-	-	-	38	(Liu <i>et al.</i> 2017)
Nano silica /PDA ^(b) /PEI ^(c) /PP coated hollow fiber	Mussel-inspired/surface coating modification	3.5 wt% NaCl	80	-95 kPa	500	-	99.92	15	(Zhong <i>et al.</i> 2017)
iPP ^(d) /EVA ^(e) /NWF ^(f) flat sheet	Blending/TIPs	3 wt% NaCl	70	3 kPa	208	120	99.9	27.6	(Tang <i>et al.</i> 2016)
Si ^(g) /PP hollow fiber	Surface coating modification	3.5 wt% NaCl	25	0.3 kPa	-	-	-	0.04	(Xu <i>et al.</i> 2006)
PTFE hollow fiber	Cold pressing method	3 wt% NaCl	70	-0.095 Mpa	170	128.5	99.9	9.5	(Zhu <i>et al.</i> 2013)
FEP hollow fiber ^(h)	Melt-stretching spinning	3.5 wt% NaCl	90	-0.09 Mpa	54	116.7	99	7	(Chen <i>et al.</i> 2015)
Fuorinated hydrocarbon hollow fiber	Commercial product	1 wt% NaCl	85	Atmosphere	-	126	99	19	(Zhang <i>et al.</i> 2010)
Fsi/PPESK hollow fiber ⁽ⁱ⁾	Surface coating /NIPs	0.5 wt% NaCl	40	-0.078 Mpa	18	110	99	3.5	(Jin <i>et al.</i> 2008)
Si/PPESK hollow fiber ⁽ⁱ⁾	Surface coating /NIPs	0.5 wt% NaCl	40	-0.078 Mpa	12	128	94.6	3.7	(Jin <i>et al.</i> 2008)
PVDF/Ultem ^(k) dual-layer hollow fiber	Co-extrusion /NIPs method	3.5 wt% NaCl	70	2 kPa	210	126.5	-	45.8	(Zuo <i>et al.</i> 2017b)
PVDF hollow fiber	NIPs method	8 wt% NaCl	80	-	-	-	-	17.5	(Sun <i>et al.</i> 2014)
Hyflon AD60/PVDF hollow fiber ^(l)	Surface coating /NIPs	3.5 wt% NaCl	70	-0.09 Mpa	700	138.9	99.9	9.0	(Tong <i>et al.</i> 2016)
3-layers PVDF hollow fiber	Co-extrusion /NIPs method	3.5 wt% NaCl	60	20 mbar	300	-	-	26.5	(Zuo <i>et al.</i> 2017a)
PVDF/SiO ₂ flat sheet	NIPS	3.5 wt% NaCl	27	-	2.9	94	99.98	2.7	(Efome <i>et al.</i> 2015)
PVDF composite fiber	Surface coating /NIPs	3.5 wt% NaCl	50	31.3 kPa	223	130.8	99.99	12.2	This work

(a) PP-Polypropylene; (b) PDA-polydopamine; (c) PEI- polyethyleneimine; (d) iPP-Isotactic polypropylene; (e) EVA-Ethylene vinyl acetate; (f) NWF-nonwoven fabric; (g) Si-Silicone rubber; (h) FEP-Poly(tetrafluoroethylene-co-hexafluoropropylene); (i) Fsi-polytrifluoropropylsiloxane; (j) PPESK-Poly(phthalazinone ether sulfone ketone); (k) Ultem[®]-Polyetherimide; (l) Hyflon AD60-Copolymer of tetrafluoroethylene (TFE) and 2,2,4- trifluoro- 5-trifluoro methoxy- 1,3-dioxole (TTD)

the water flux was between 1-10 kg·m⁻²·h⁻¹. By comparison, the PVDF hollow fiber composite membranes developed in this work exhibited the moderate performance under a high permeation pressure and a low feed temperature. The effects

of operation conditions on the VMD performance of PVDF composite membrane are under way to pursue even better separation performance. Therefore, this study may provide useful insights to prepared high-performance PVDF hollow fiber membranes for VMD applications.

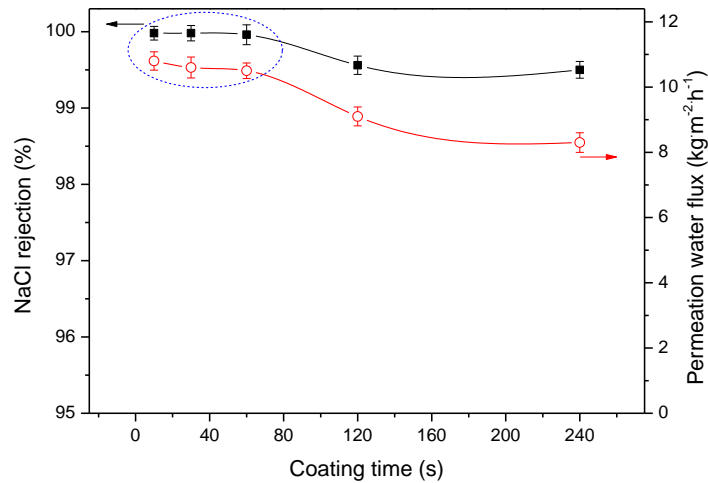


Fig. 9 Effect of coating time on the VMD performance of PVDF composite membrane

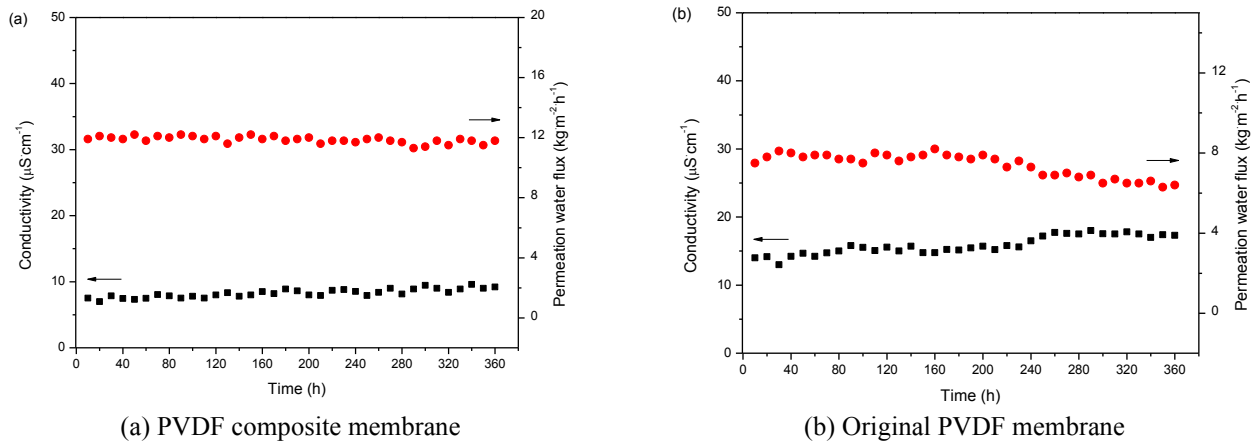


Fig. 10 Long-term VMD performance of different PVDF hollow fiber membranes

3.6 Effect of coating time on VMD performance

Fig. 9 showed the variations of coating time on the VMD performance of PVDF composite membrane (2#). It could be seen from Fig. 9 that VMD permeability decreased slowly with the extension of coating time and then went down dramatically when the coating time became longer than 60 s. When the coating time was short, the PVDF-HFP dilute dope solution deposited only on the surface of PVDF support membrane, and the effective enhancement of membrane surface hydrophobicity could be obtained. Therefore, the separation performance had no obvious variations as shown in Fig. 9. However, when the coating time was longer than 60 s, more PVDF-HFP dilute dope solution penetrated into PVDF membrane pores and the transport resistance increased, leading to a low permeability. Thus, the coating time in the range of 10–60 s was desirable during the preparation of PVDF hollow fiber composite membrane.

3.7 Long-term performance of different PVDF hollow fiber membranes

Fig. 10 showed the permeation water flux and production water conductivity of the original PVDF

membrane and PVDF hollow fiber composite membranes (2#). It could be seen from Fig. 10(a) that with the extension of the operation time PVDF composite membrane showed a stable VMD performance. Membrane permeation water flux and production conductivity kept almost unchanged with the data of 8 $\mu\text{S cm}^{-1}$ and 12 $\text{kg m}^{-2}\text{h}^{-1}$, respectively. By contrast, the original PVDF membrane VMD performance basically remained stable in the first 210 h as illustrated in Fig. 10(b). Afterwards, membrane experienced an obvious flux decrease accompanied by a slow conductivity increase. These results suggested PVDF membrane suffered fouling which probably was derived from the micropore wetting. The stable separation performance of PVDF composite membrane could be attributed to the special micro-nano structure on the PVDF composite membrane surface which played the similar self-cleaning effect of the lotus leaf surface. These results indicated that the PVDF-HFP coating effectively enhanced the stability of the PVDF hollow fiber membranes for VMD application.

4. Conclusions

The hydrophobic PVDF hollow fiber composite membranes were prepared by coating PVDF-HFP dilute

solution on the outside surface of PVDF support membrane. 35 g·L⁻¹ NaCl aqueous solution was used to simulate the seawater and used as the feed solution in VMD process. Surface hydrophobicity of the PVDF hollow fiber membrane was significantly improved. The surface structure played an important role in membrane separation performance in VMD test. The vapour flux reached a maximum when PVDF-HFP concentration in the dilute solution was 5 wt%. This was attributed to the well configuration of micro-nano rods which was similar with the dual micro-nano structure on the lotus leaf. The salt rejection was kept at 99.99 % during the long-term run operation of PVDF composite membrane for 360 h. These results indicated that PVDF hollow fiber composite membrane is a promising candidate for VMD process. The effects of operation conditions on the VMD performance of PVDF composite membrane are under way to pursue even better separation performance and will be reported in due course.

Acknowledgments

The authors gratefully acknowledge the funding for the Project supported by the Program for Key Research Project of Higher Education of Henan Province (No. 18A540001) and the Training plan for Young Scholar in Colleges and Universities in Henan Province (No. 2017GGJS151, and No. 2018GGJS151) and the Central Plains Thousand People Program-Top Young Talents in Central Plains (No, ZYQR201810135).

References

- Alkhudhiri, A., Darwish, N. and Hilal, N. (2012), "Membrane distillation, a comprehensive review", *Desalination.*, **287**, 2-18.
- Ameen, S., Park, D.R., Akhtar, M.S. and Shin, H.S. (2016), "Lotus-leaf like ZnO nanostructures based electrode for the fabrication of ethyl acetate chemical sensor", *Mater. Lett.*, **164**, 562-566.
- Chang, J., Zuo, J., Lu, K.J. and Chung, T.S. (2019), "Membrane development and energy analysis of freeze desalination-vacuum membrane distillation hybrid systems powered by LNG regasification and solar energy", *Desalination.*, **449**, 16-25.
- Chang, H.H., Tsai, C.H., Wei, H.C. and Cheng, L.P. (2014), "Effect of structure of PVDF membranes on the performance of membrane distillation", *Membr. Water Treat.*, **5**(1), 41-56.
- Chen, F.F., Jia, Y., Wang, Q.G., Cao, X.B., Li, Y.H., Lin, Y., Cui, X. and Wei, J.Q. (2018), "Strong and super-hydrophobic hybrid carbon nanotube films with superior loading capacity", *Carbon.*, **137**, 88-92.
- Chen, K.K., Xiao, C.F., Huang, Q.L., Liu, H., Liu, H.L., Wu, Y.J. and Liu, Z. (2015), "Study on vacuum membrane distillation (VMD) using FEP hollow fiber membrane", *Desalination.*, **375**, 24-32.
- Drioli, E., Ali, A., Simone, S., Macedonio, F., Al-Jlil, S.A., Al-Shabonah, F.S., Al-Romaih, H.S., Al-Harbi, A., Figoli, O. and Criscuoli, A. (2013), "Novel PVDF hollow fiber membranes for vacuum and direct contact membrane distillation applications", *Sep. Purif. Technol.*, **115**, 27-38.
- Edwie, F., Teoh, M.M. and Chung, T.S. (2012), "Effects of additives on dual-layer hydrophobic-hydrophilic PVDF hollow fiber membranes for membrane distillation and continuous performance", *Chem. Eng. Sci.*, **68**, 567-578.
- Efome, J.E., Baghbanzadeh, M., Rana, D., Matsuura, T. and Lan, C.Q. (2015), "Effects of superhydrophobic SiO₂ nanoparticles on the performance of PVDF flat sheet membranes for vacuum membrane distillation", *Desalination.*, **373**, 47-57.
- Fang, H., Gao, J.F., Wang, H.T. and Chen, C.S. (2012), "Hydrophobic porous alumina hollow fiber for water desalination via membrane distillation process", *J. Membr. Sci.*, **403-404**, 41-46.
- Ganesh, B.M., Isloor, A.M. and Ismail, A.F. (2013), "Enhanced hydrophilicity and salt rejection study of graphene oxide-polysulfone mixed matrix membrane", *Desalination.*, **313**, 199-207.
- García-Fernández, L., García-Payo, M.C. and Khayet, M. (2014), "Effects of mixed solvents on the structural morphology and membrane distillation performance of PVDF-HFP hollow fiber membranes", *J. Membr. Sci.*, **468**, 324-338.
- García-Fernández, L., García-Payo, M.C. and Khayet, M. (2017a), "Mechanism of formation of hollow fiber membranes for membrane distillation: 1. Inner coagulation power effect on morphological characteristics", *J. Membr. Sci.*, **542**, 456-468.
- García-Fernández, L., García-Payo, M.C. and Khayet, M. (2017b), "Mechanism of formation of hollow fiber membranes for membrane distillation: 2. Outer coagulation power effect on morphological characteristics", *J. Membr. Sci.*, **542**, 469-481.
- García-Payo, M.C., Essalhi, M. and Khayet, M. (2009), "Preparation and characterization of PVDF-HFP copolymer hollow fiber membranes for membrane distillation", *Desalination.*, **245**, 469-473.
- García-Payo, M.C., Essalhi, M. and Khayet, M. (2010), "Effects of PVDF-HFP concentration on membrane distillation performance and structural morphology of hollow fiber membranes", *J. Membr. Sci.*, **347**, 209-219.
- Gryt, M. (2013), "Osmotic membrane distillation with continuous regeneration of stripping solution by natural evaporation", *Membr. Water Treat.*, **4**(4), 223-236.
- Guo, H., Peng, C.S., Ma, W.F., Yuan, H.T. and Yang, K. (2017), "Study on the heat and mass transfer in ultrasonic assisting vacuum membrane distillation", *Membr. Water Treat.*, **8**(3), 293-310. <http://dx.doi.org/10.12989/mwt.2017.8.3.293>.
- Jin, Z., Yang, D.L., Zhang, S.H. and Jian, X.G. (2008), "Hydrophobic modification of poly(phthalazinone ether sulfone ketone) hollow fiber membrane for vacuum membrane distillation", *J. Membr. Sci.*, **310**, 20-27. <https://doi.org/10.1016/j.memsci.2007.10.021>.
- Khayet, M., Cojocaru, C., Essalhi, M., García-Payo, M.C. and Arribas, P.L. (2012), "Hollow fiber spinning experimental design and analysis of defects for fabrication of optimized membranes for membrane distillation", *Desalination.*, **287**, 146-158. <https://doi.org/10.1016/j.desal.2011.06.025>.
- Kim, S., Park, K.Y. and Cho, J.W. (2017), "Evaluation of the efficiency of cleaning method in direct contact membrane distillation of digested livestock wastewater", *Membr. Water Treat.*, **8**(2), 113-123. <http://dx.doi.org/10.12989/mwt.2017.8.2.113>.
- Kim, S.J., Kim, T.H., Kong, J.H., Kim, Y.S., Cho, C.R., Kim, S.H., Lee, D.W., Park, J.K., Lee, D.Y. and Kim, J.M. (2012), "Dual-scale artificial lotus leaf fabricated by fully nonlithographic simple approach based on sandblasting and anodic aluminum oxidation techniques", *Appl. Surf. Sci.*, **263**, 648-654.
- Li, H.B., Zhang, H.X., Qin, X.H. and Shi, W.Y. (2017), "Improved separation and antifouling properties of thin-film composite nanofiltration membrane by the incorporation of cGO", *Appl. Surf. Sci.*, **407**, 260-275. <https://doi.org/10.1016/j.apsusc.2017.02.204>.
- Liu, J., Wang, Q., Han, L. and Li, B.A. (2017), "Simulation of heat and mass transfer with cross-flow hollow fiber vacuum membrane distillation, The influence of fiber arrangement",

- Chem. Eng. Res. Des.*, **119**, 12-22. <https://doi.org/10.1016/j.cherd.2017.01.013>.
- Loussif, N. and Orfi, J. (2016), "Comparative study of air gap, direct contact and sweeping gas membrane distillation configurations", *J. Membr. Sci.*, **7**(1), 71-86. <http://dx.doi.org/10.12989/mwt.2016.7.1.071>.
- Lu, K.J., Zuo, J. and Chung, T.S. (2016), "Tri-bore PVDF hollow fibers with a super-hydrophobic coating for membrane distillation", *J. Membr. Sci.*, **514**, 165-175. <https://doi.org/10.1016/j.memsci.2016.04.058>.
- Lu, K.J., Zuo, J., Chang, J., Kuan, H.N. and Chung, T.S. (2018), "Omniphobic Hollow-Fiber Membranes for Vacuum Membrane Distillation", *Environ. Sci. Technol.*, **52**, 4472-4480. <https://doi.org/10.1021/acs.est.8b00766>.
- Meng, S., Mansouri, J., Ye, Y. and Chen, V. (2014), "Effect of templating agents on the properties and membrane distillation performance of TiO₂-coated PVDF membranes", *J. Membr. Sci.*, **450**, 48-59. <https://doi.org/10.1016/j.memsci.2013.08.036>.
- Mierzwa, J.C., Vecitis, C.D., Carvalho, J., Arieta, V. and Verlage, M. (2012), "Anion dopant effects on the structure and performance of polyethersulfone membranes", *J. Membr. Sci.*, **421-422**, 91-102. <https://doi.org/10.1016/j.memsci.2012.06.039>.
- Pangarkar, B.L., Deshmukh, S.K. and Thorat, P.V. (2017), "Multi-effect air gap membrane distillation process for pesticide wastewater treatment", *Membr. Water Treat.*, **8**(6), 529-541.
- Peng, Y.L., Fan, H.W., Dong, Y.J., Song, Y.N. and Han, H. (2012a) "Effects of exposure time on variations in the structure and hydrophobicity of polyvinylidene fluoride membranes prepared via vapor-induced phase separation", *Appl. Surf. Sci.*, **258**, 7872-7881. <https://doi.org/10.1016/j.apsusc.2012.04.108>.
- Peng, Y.L., Fan, H.W., Ge, J., Wang, S.B., Chen, P. and Jiang, Q. (2012b) "The effects of processing conditions on the surface morphology and hydrophobicity of polyvinylidene fluoride membranes prepared via vapor-induced phase separation", *Appl. Surf. Sci.*, **263**, 737-744. <https://doi.org/10.1016/j.apsusc.2012.09.152>.
- Racz, G., Kerker, S., Schmitz, O., Schnabel, B., Kovacs, Z., Vatai, G., Ebrahimi, M. and Czermak, P. (2015), "Experimental determination of liquid entry pressure (LEP) in vacuum membrane distillation for oily wastewaters", *Membr. Water Treat.*, **6**(3), 237-249. <http://dx.doi.org/10.12989/mwt.2015.6.3.237>.
- Shafiei, M. and Alpas, A.T. (2009), "Nanocrystalline nickel films with lotus leaf texture for superhydrophobic and low friction surfaces", *Appl. Surf. Sci.*, **256**, 710-719. <https://doi.org/10.1016/j.apsusc.2009.08.047>.
- Sun, A.C., Kosar, W., Zhang, Y.F. and Feng, X.S. (2014), "Vacuum membrane distillation for desalination of water using hollow fiber membranes", *J. Membr. Sci.*, **455**, 131-142. <https://doi.org/10.1016/j.memsci.2013.12.055>.
- Tang, N., Feng, C.L., Han, H.Y., Hua, X.X., Zhang, L., Xiang, J., Cheng, P.G., Du, W. and Wang, X.K. (2016), "High permeation flux polypropylene/ethylene vinyl acetate co-blending membranes via thermally induced phase separation for vacuum membrane distillation desalination", *Desalination.*, **394**, 44-55. <https://doi.org/10.1016/j.desal.2016.04.024>.
- Tang, Y.D., Li, N., Liu, A.J., Ding, S.K., Yi, C.H. and Liu, H. (2012), "Effect of spinning conditions on the structure and performance of hydrophobic PVDF hollow fiber membranes for membrane distillation", *Desalination.*, **287**, 326-339. <https://doi.org/10.1016/j.desal.2011.11.045>.
- Teoh, M.M. and Chung, T.S. (2009), "Membrane distillation with hydrophobic macrovoid-free PVDF-PTFE hollow fiber membranes", *Sep. Purif. Technol.*, **66**, 229-236. <https://doi.org/10.1016/j.seppur.2009.01.005>.
- Tong, D.Q., Wang, X.Z., Ali, M., Lan, C.Q., Wang, Y., Drioli, E., Wang, Z.H. and Cui, Z.L. (2016), "Preparation of Hyflon AD60/PVDF composite hollow fiber membranes for vacuum membrane distillation", *Sep. Purif. Technol.*, **157**, 1-8. <https://doi.org/10.1016/j.seppur.2015.11.026>.
- Wang, J., Zheng, L.B., Wu, Z.J., Zhang, Y. and Zhang, X.H. (2016), "Fabrication of hydrophobic flat sheet and hollow fiber membranes from PVDF and PVDF-CTFE for membrane distillation", *J. Membr. Sci.*, **497**, 183-193. <https://doi.org/10.1016/j.memsci.2015.09.024>.
- Wu, B., Tan, X.Y., Li, K. and Teo, W.K. (2006), "Removal of 1,1,1-trichloroethane from water using a polyvinylidene fluoride hollow fiber membrane module, Vacuum membrane distillation operation", *Sep. Purif. Technol.*, **52**, 301-309. <https://doi.org/10.1016/j.seppur.2006.05.013>.
- Xu, J.L., Furuswa, M. and Ito, A. (2006), "Air-sweep vacuum membrane distillation using fine silicone, rubber, hollow-fiber membranes", *Desalination.*, **191**, 223-231. <https://doi.org/10.1016/j.desal.2005.08.015>.
- Xu, J.L., Bettahalli, N.M.S., Chisca, S., Khalid, M.K., Ghaffour, N., Vilagines, R. and Nunes, S.P. (2018), "Polyoxadiazole hollow fibers for produced water treatment by direct contact membrane distillation", *Desalination.*, **432**, 32-39. <https://doi.org/10.1016/j.desal.2017.12.014>.
- Xu, Z.H., Liu, Z., Song, P.F., Xiao, C.F., Jian, Z., Bonyadi, S. and Chung, T.S. (2015), "Exploring the potential of commercial polyethylene membranes for desalination by membrane distillation", *J. Membr. Sci.*, **497**, 239-247. <https://doi.org/10.1016/j.memsci.2015.09.038>.
- Xu, Z.H., Liu, Z., Song, P.F. and Xiao, C.F. (2017), "Fabrication of super-hydrophobic polypropylene hollow fiber membrane and its application in membrane distillation", *Desalination.*, **414**, 10-17. <https://doi.org/10.1016/j.desal.2017.03.029>.
- Yan, H.Q., Lu, X.L., Wu, C.R., Sun, X.C. and Tang, W.Y. (2017), "Fabrication of a super-hydrophobic polyvinylidene fluoride hollow fiber membrane using a particle coating process", *J. Membr. Sci.*, **533**, 130-140. <https://doi.org/10.1016/j.memsci.2017.03.033>.
- Zhang, J.H., Li, J.D., Duke, M., Xie, Z.L. and Gray, S. (2010), "Performance of asymmetric hollow fibre membranes in membrane distillation under various configurations and vacuum enhancement", *J. Membr. Sci.*, **362**, 517-528. <https://doi.org/10.1016/j.memsci.2010.07.004>.
- Zheng, Z.R., Gu, Z.Y., Huo, R.T. and Ye, Y.H. (2009), "Superhydrophobicity of polyvinylidene fluoride membrane fabricated by chemical vapor deposition from solution", *Appl. Surf. Sci.*, **255**, 7263-7267. <https://doi.org/10.1016/j.apsusc.2009.03.084>.
- Zhong, W.W., Hou, J.W., Yang, H.C. and Chen, V. (2017), "Superhydrophobic membranes via facile bio-inspired mineralization for vacuum membrane distillation", *J. Membr. Sci.*, **540**, 98-107. <https://doi.org/10.1016/j.memsci.2017.06.033>.
- Zhu, H.L., Wang, H.J., Wang, F., Guo, Y.H., Zhang, H.P. and Chen, J.Y. (2013), "Preparation and properties of PTFE hollow fiber membranes for desalination through vacuum membrane distillation", *J. Membr. Sci.*, **446**, 145-153. <https://doi.org/10.1016/j.memsci.2013.06.037>.
- Zuo, J. and Chung, T.S. (2017a), "PVDF hollow fibers with novel sandwich structure and superior wetting resistance for vacuum membrane distillation", *Desalination.*, **417**, 94-101. <https://doi.org/10.1016/j.desal.2017.05.022>.
- Zuo, J., Chung, T.S., Brien, G.S.O. and Kosar, W. (2017b), "Hydrophobic/hydrophilic PVDF/Ultem® dual-layer hollow fiber membranes with enhanced mechanical properties for vacuum membrane distillation", *J. Membr. Sci.*, **523**, 103-110. <https://doi.org/10.1016/j.memsci.2016.09.030>.